

Supporting Information

Poly(ionic liquid)s with unique adsorption-swelling ability toward epoxides for efficient atmospheric CO₂ conversion under cocatalyst-/metal-/solvent-free conditions

Bihua Chen, Shiguo Zhang* and Yan Zhang*

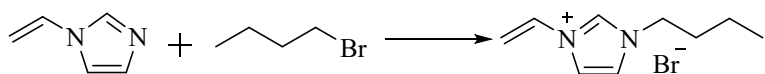
College of Materials Science and Engineering, Hunan University, Changsha 410082,
Hunan, China

*Corresponding author.

E-mail addresses: zhangsg@hnu.edu.cn (S. Zhang), zyan1980@hnu.edu.cn (Y. Zhang).

1. Synthesis of ionic liquid monomers

1.1. Synthesis of 1-vinyl-3-butylimidazolium bromide ($[VC4Im]Br$)

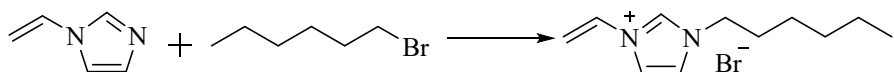


Scheme S1 Synthetic route of $[VC4Im]Br$.

1-Vinylimidazole (50 mmol) and 1-bromobutane (55 mmol) were added into a 100 mL round-bottom flask. The mixture was stirred at 50 °C for 24 h. The crude product was washed with diethyl ether until 1-vinylimidazole was not detected in the washing liquid by thin layer chromatography (TLC) and then dried under vacuum at 40 °C for 12 h. $[VC4Im]Br$ was obtained at a yield of approximately 80 % and was structurally characterized by NMR spectroscopy.

1H NMR (400 MHz, DMSO-d₆, TMS) δ (ppm): 9.66 (s, 1H), 8.24 (s, 1H), 7.97 (s, 1H), 7.32 (dd, J = 15.6, 8.8 Hz, 1H), 5.99 (dd, J = 15.6, 2.4 Hz, 1H), 5.42 (dd, J = 8.8, 2.0 Hz, 1H), 4.22 (t, J = 7.2 Hz, 2H), 1.85–1.77 (m, 2H), 1.33–1.24 (m, 2H), 0.90 (t, J = 7.2 Hz, 3H); ^{13}C NMR (100 MHz, DMSO-d₆, TMS) δ (ppm): 135.77, 129.32, 123.72, 119.65, 109.09, 49.38, 31.53, 19.26, 13.77.

1.2. Synthesis of 1-vinyl-3-hexylimidazolium bromide ($[VC6Im]Br$)

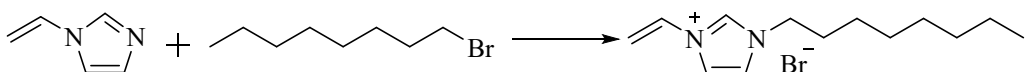


Scheme S2 Synthetic route of $[VC6Im]Br$.

Similarly, the ionic liquid monomer $[VC6Im]Br$ was synthesized *via* the reaction of 1-vinylimidazole with 1-bromohexane. $[VC6Im]Br$ was obtained at a yield of approximately 94 % and was structurally characterized by NMR spectroscopy.

1H NMR (400 MHz, DMSO-d₆, TMS) δ (ppm): 9.71 (s, 1H), 8.27 (s, 1H), 8.00 (s, 1H), 7.34 (dd, J = 15.6, 8.8 Hz, 1H), 6.00 (dd, J = 15.6, 2.0 Hz, 1H), 5.41 (dd, J = 8.8, 2.4 Hz, 1H), 4.22 (t, J = 7.2 Hz, 2H), 1.85–1.78 (m, 2H), 1.29–1.21 (m, 6H), 0.84 (t, J = 6.6 Hz, 3H); ^{13}C NMR (100 MHz, DMSO-d₆, TMS) δ (ppm): 135.76, 129.33, 123.71, 119.64, 109.08, 49.64, 31.01, 29.51, 25.60, 22.32, 14.30.

1.3. Synthesis of 1-vinyl-3-octylimidazolium bromide ([VC8Im]Br)

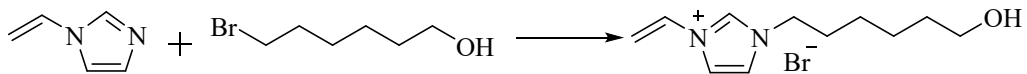


Scheme S3 Synthetic route of [VC8Im]Br.

Similarly, the ionic liquid monomer [VC8Im]Br was synthesized *via* the reaction of 1-vinylimidazole with 1-bromo-octane. [VC8Im]Br was obtained at a yield of approximately 78 % and was structurally characterized by NMR spectroscopy.

¹H NMR (400 MHz, DMSO-d₆, TMS) δ (ppm): 9.79 (s, 1H), 8.30 (s, 1H), 8.02 (s, 1H), 7.36 (dd, *J* = 15.6, 8.8 Hz, 1H), 6.02 (dd, *J* = 15.6, 2.0 Hz, 1H), 5.40 (dd, *J* = 8.8, 2.0 Hz, 1H), 4.23 (t, *J* = 7.2 Hz, 2H), 1.85–1.78 (m, 2H), 1.28–1.17 (m, 10H), 0.82 (t, *J* = 6.6 Hz, 3H); ¹³C NMR (100 MHz, DMSO-d₆, TMS) δ (ppm): 135.75, 129.31, 123.71, 119.64, 109.06, 49.65, 31.62, 29.57, 28.92, 28.81, 25.95, 22.51, 14.39.

1.4. Synthesis of 1-vinyl-3-(1-hydroxyhexyl)imidazolium bromide ([VHC6Im]Br)



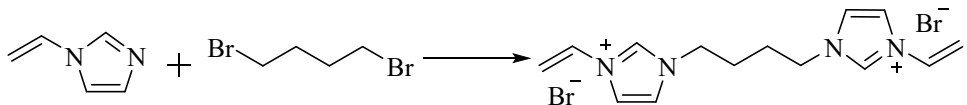
Scheme S4 Synthetic route of [VHC6Im]Br.

Similarly, the ionic liquid monomer [VHC6Im]Br was synthesized *via* the reaction of 1-vinylimidazole with 6-bromo-1-hexanol. [VHC6Im]Br was obtained at a yield of approximately 73 % and was structurally characterized by NMR spectroscopy.

¹H NMR (400 MHz, DMSO-d₆, TMS) δ (ppm): 9.60 (s, 1H), 8.23 (s, 1H), 7.96 (s, 1H), 7.31 (dd, *J* = 15.6, 8.8 Hz, 1H), 5.98 (dd, *J* = 15.6, 2.0 Hz, 1H), 5.42 (dd, *J* = 8.8, 2.0 Hz, 1H), 4.36 (s, 1H), 4.20 (t, *J* = 7.2 Hz, 2H), 3.37 (t, *J* = 6.2 Hz, 2H), 1.86–1.79 (m, 2H), 1.44–1.23 (m, 6H); ¹³C NMR (100 MHz, DMSO-d₆, TMS) δ (ppm): 135.76, 129.33, 123.70, 119.63, 109.08, 60.93, 49.64, 32.64, 29.61, 25.84, 25.35.

2. Synthesis of crosslinkers

2.1. Synthesis of 1,4-di(3-vinylimidazolium)butane dibromide ($[C4(VIm)_2]Br_2$)

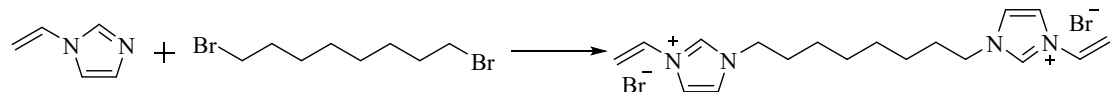


Scheme S5 Synthetic route of $[C4(VIm)_2]Br_2$.¹

1-Vinylimidazole (41 mmol) and 1,4-dibromobutane (20 mmol) were dissolved in CHCl₃ (10 mL) in a 100 mL round-bottom flask. The mixture was stirred under reflux conditions for 24 h. After the reaction finished, the upper phase was removed, and the lower phase was washed with diethyl ether until 1-vinylimidazole was not detected in the washing liquid by TLC. $[C4(VIm)_2]Br_2$ was obtained at a yield of approximately 95 % and was structurally characterized by NMR spectroscopy.

¹H NMR (400 MHz, DMSO-d₆, TMS) δ (ppm): 9.66 (s, 2H), 8.24 (s, 2H), 7.98 (s, 2H), 7.33 (dd, *J* = 15.6, 8.8 Hz, 2H), 5.98 (dd, *J* = 15.6, 2.4 Hz, 2H), 5.43 (dd, *J* = 8.8, 2.0 Hz, 2H), 4.33–4.25 (m, 4H), 1.92–1.82 (m, 4H); ¹³C NMR (100 MHz, DMSO-d₆, TMS) δ (ppm): 135.91, 129.34, 123.70, 119.63, 109.17, 48.86, 26.19.

2.2. Synthesis of 1,8-di(3-vinylimidazolium)octane dibromide ($[C8(VIm)_2]Br_2$)



Scheme S6 Synthetic route of $[C8(VIm)_2]Br_2$.

Similarly, the crosslinker $[C8(VIm)_2]Br_2$ was synthesized *via* the reaction of 1-vinylimidazole with 1,8-dibromo-octane. $[C8(VIm)_2]Br_2$ was obtained at a yield of approximately 97 % and was structurally characterized by NMR spectroscopy.

¹H NMR (400 MHz, DMSO-d₆, TMS) δ (ppm): 9.62 (s, 2H), 8.23 (s, 2H), 7.96 (s, 2H), 7.32 (dd, *J* = 15.6, 8.8 Hz, 2H), 5.98 (dd, *J* = 15.6, 2.0 Hz, 2H), 5.42 (dd, *J* = 8.8, 2.4 Hz, 2H), 4.20 (t, *J* = 7.2 Hz, 4H), 1.86–1.79 (m, 4H), 1.34–1.20 (m, 8H); ¹³C NMR (100 MHz, DMSO-d₆, TMS) δ (ppm): 135.70, 129.29, 123.70, 119.62, 109.13, 49.62, 29.50, 28.58, 25.83.

3. Synthesis of the PILs

Table S1 The yields of the PILs.

PIL	Yield (%)
P-[VC6Im]Br-DVB-10%	91
P-[VC6Im]Br-C4-10%	79
P-[VC6Im]Br-C8-10%	79
P-[VC4Im]Br-C8-10%	96
P-[VC8Im]Br-C8-10%	82
P-[VHC6Im]Br-C8-10%	88
P-[VC6Im]Br-C8-5%	77
P-[VC6Im]Br-C8-20%	81

4. Adsorption-swelling rules of the PILs

Table S2 The parameters of solvents.²

Solvent	δ (MPa ^{1/2})	Hansen solubility parameter		
		δ_D (MPa ^{1/2})	δ_P (MPa ^{1/2})	δ_H (MPa ^{1/2})
Water	47.8	15.5	16.0	42.3
Ethylene glycol	33.0	17.0	11.0	26.0
Methanol	29.6	15.1	12.3	22.3
DMSO	26.7	18.4	16.4	10.2
Ethanol	26.5	15.8	8.8	19.4
DMF	24.9	17.4	13.7	11.3
Chloroform	18.9	17.8	3.1	5.7
<i>n</i> -Hexane	14.9	14.9	0	0

Data from reference 2.

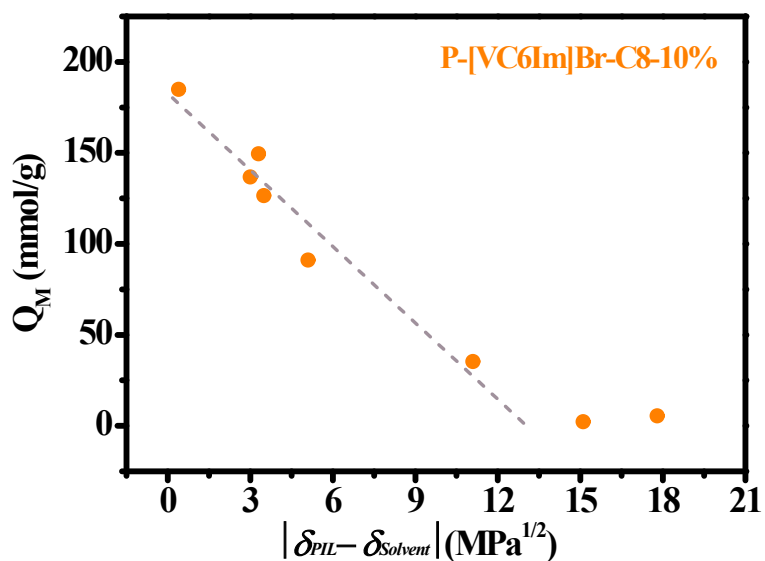


Fig. S1 Relationship between the Q_M value of P-[VC6Im]Br-C8-10% and the absolute value of the difference of solubility parameters between P-[VC6Im]Br-C8-10% and solvent ($|\delta_{PIL} - \delta_{Solvent}|$).

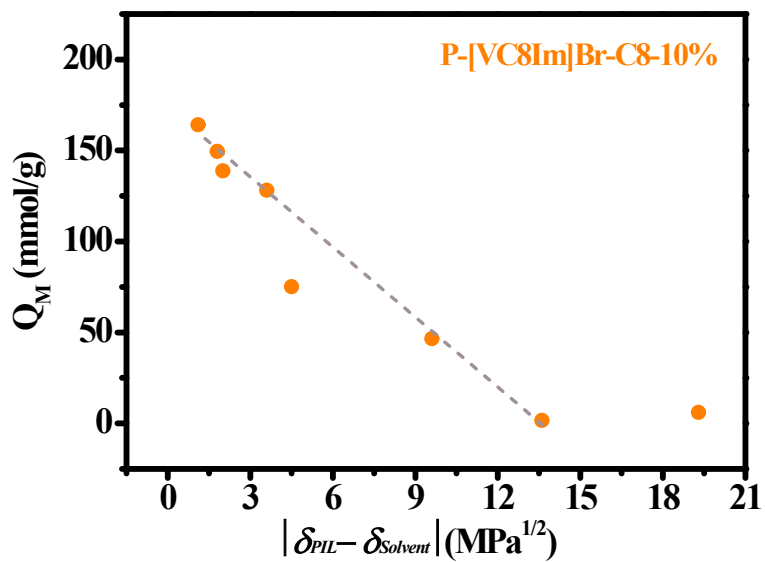


Fig. S2 Relationship between the Q_M value of P-[VC8Im]Br-C8-10% and the absolute value of the difference of solubility parameters between P-[VC8Im]Br-C8-10% and solvent ($|\delta_{PIL} - \delta_{Solvent}|$).

5. Characterizations of the PILs

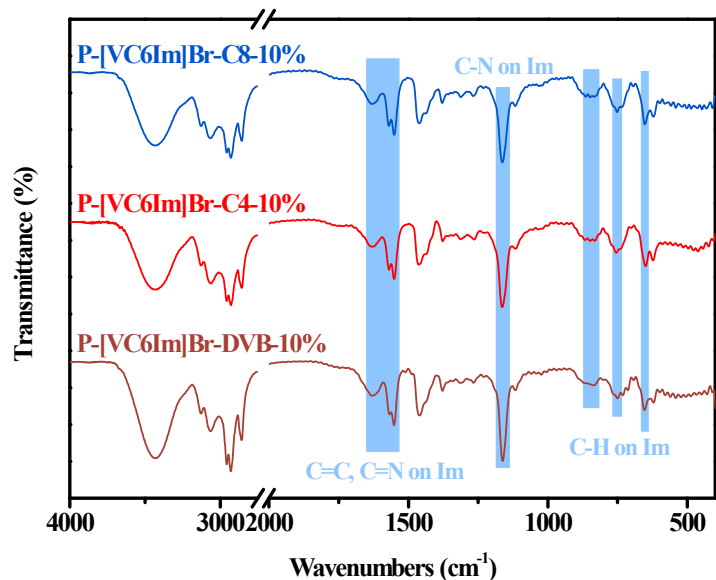


Fig. S3 FT-IR spectra of P-[VC6Im]Br-DVB-10%, P-[VC6Im]Br-C4-10%, and P-[VC6Im]Br-C8-10%. (Wavenumber from 2750 to 2000 cm⁻¹ was broken.)

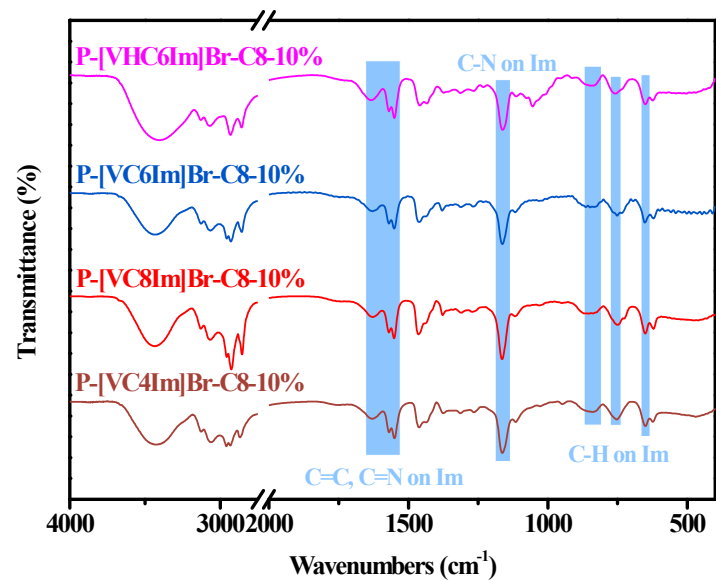


Fig. S4 FT-IR spectra of P-[VC4Im]Br-C8-10%, P-[VC8Im]Br-C8-10%, P-[VC6Im]Br-C8-10%, and P-[VHC6Im]Br-C8-10%. (Wavenumber from 2750 to 2000 cm⁻¹ was broken.)

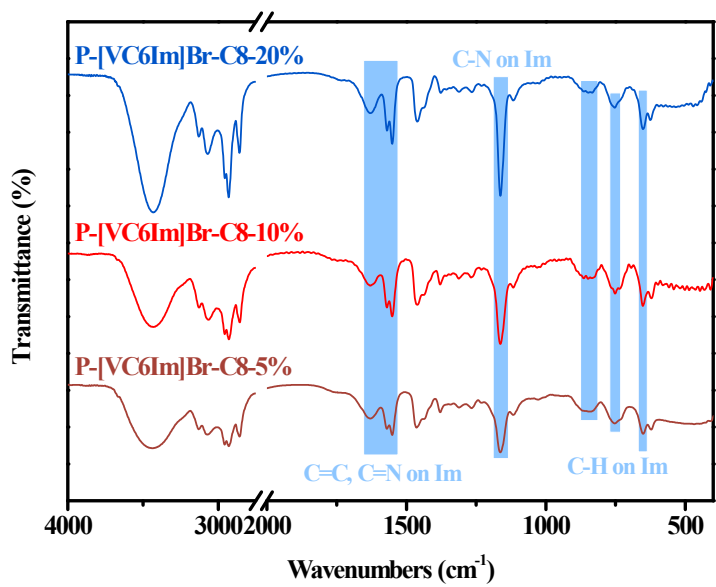


Fig. S5 FT-IR spectra of P-[VC6Im]Br-C8-5%, P-[VC6Im]Br-C8-10%, and P-[VC6Im]Br-C8-20%. (Wavenumber from 2750 to 2000 cm⁻¹ was broken.)



Fig. S6 Adsorption-swelling behaviors of P-[VC6Im]Br-C8-5% in various epoxides.

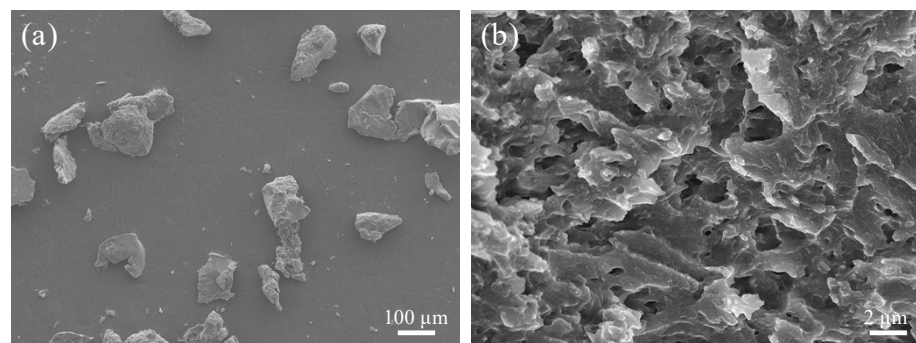


Fig. S7 SEM images of dried P-[VC6Im]Br-C8-5% sample (a) and swollen P-[VC6Im]Br-C8-5% sample after freeze-drying (b).

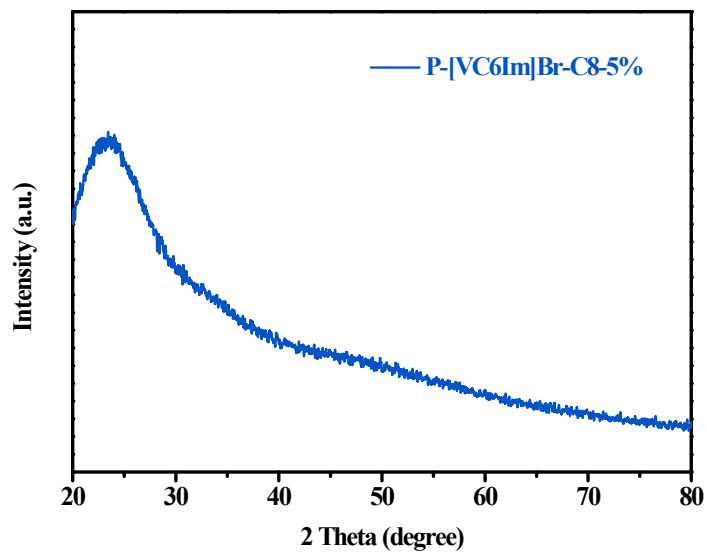


Fig. S8 XRD pattern of dried P-[VC6Im]Br-C8-5% sample.

Table S3 Textural properties of the dried PILs.

Entry	PIL	S _{BET} ^a (m ² /g)	V _{total} ^b (cm ³ /g)
1	P-[VC6Im]Br-DVB-10%	66.6	0.029
2	P-[VC6Im]Br-C4-10%	14.2	0.018
3	P-[VC6Im]Br-C8-10%	3.9	0.011
4	P-[VC4Im]Br-C8-10%	4.7	0.018
5	P-[VC8Im]Br-C8-10%	61.4	0.012
6	P-[VHC6Im]Br-C8-10%	7.6	0.021
7	P-[VC6Im]Br-C8-5%	19.5	0.031
8	P-[VC6Im]Br-C8-20%	24.3	0.034

^a The BET surface area. ^b Total pore volume.

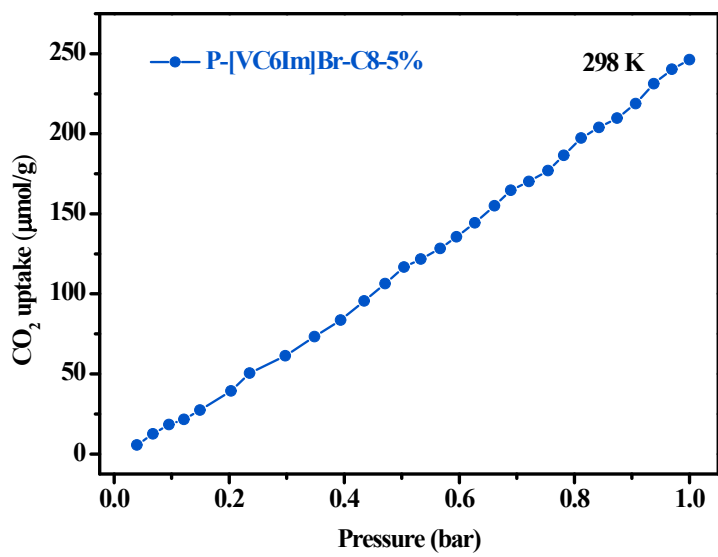


Fig. S9 CO₂ adsorption isotherm of dried P-[VC6Im]Br-C8-5% sample at 25 °C up to 1 bar.

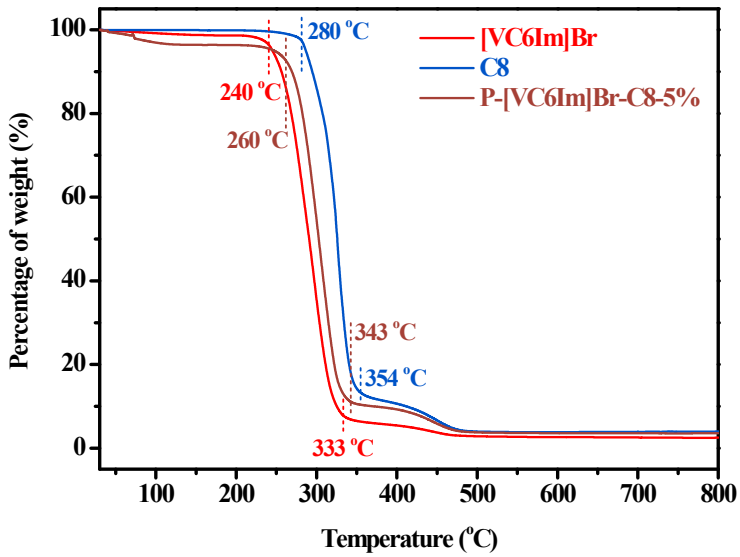


Fig. S10 TGA curves for P-[VC6Im]Br-C8-5%, [VC6Im]Br, and C8.

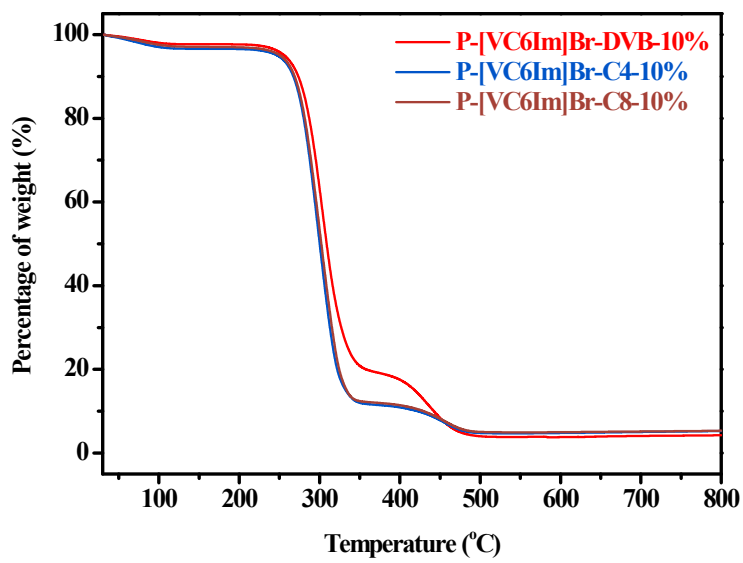


Fig. S11 TGA curves for P-[VC6Im]Br-DVB-10%, P-[VC6Im]Br-C4-10%, and P-[VC6Im]Br-C8-10%.

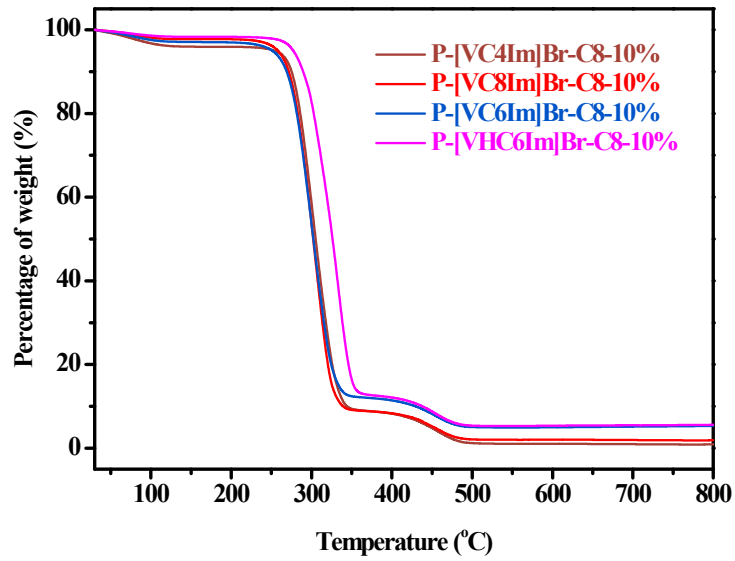


Fig. S12 TGA curves for P-[VC4Im]Br-C8-10%, P-[VC8Im]Br-C8-10%, P-[VC6Im]Br-C8-10%, and P-[VHC6Im]Br-C8-10%.

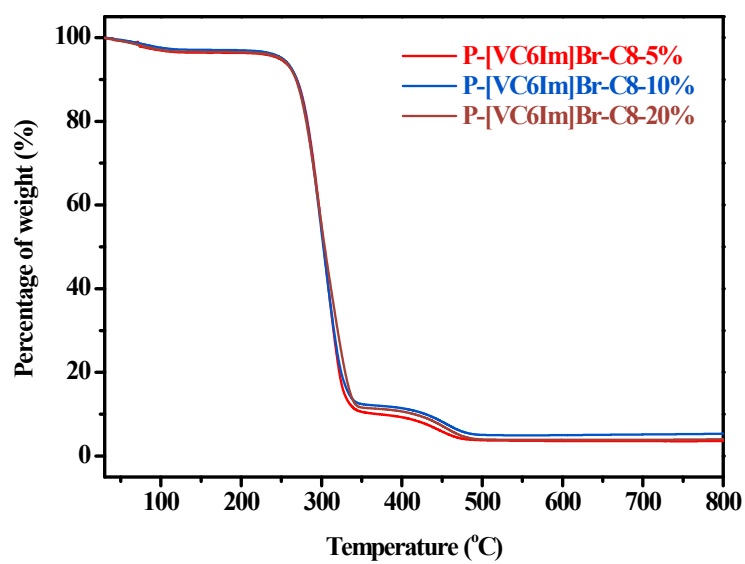


Fig. S13 TGA curves for P-[VC6Im]Br-C8-5%, P-[VC6Im]Br-C8-10%, and P-[VC6Im]Br-C8-20%.

6. Catalytic performances of various catalysts in atmospheric CO₂ cycloaddition

Table S4 Catalytic performances of various catalysts in the cycloaddition of atmospheric CO₂ with styrene oxide.^a

Entry	Catalyst	Q _M (mmol/g)	Yield (%)	Selectivity (%)
1 ^b	None	—	n.d.	—
2	P-[VC4Im]Br-C8-10%	1.6	29.5	> 99
3	P-[VHC6Im]Br-C8-10%	2.8	38.4	> 99
4	P-[VC6Im]Br-C4-10%	17.1	40.7	> 99
5	P-[VC6Im]Br-C8-20%	21.8	43.7	> 99
6	P-[VC6Im]Br-DVB-10%	23.6	51.4	> 99
7	P-[VC6Im]Br-C8-10%	40.0	67.1	> 99
8	P-[VC8Im]Br-C8-10%	63.4	68.6	> 99
9	P-[VC6Im]Br-C8-5%	54.1	75.5	> 99
10	TBABr	—	66.9	> 99
11	[VC4Im]Br	—	84.5	> 99
12	[VC6Im]Br	—	82.3	> 99
13	[VC8Im]Br	—	77.8	> 99

^a Reaction conditions: 12.5 mmol styrene oxide, 1 atm (balloon) CO₂, 2.5 mol% catalyst, 80 °C, 24 h. ^b Not detected (n.d.).

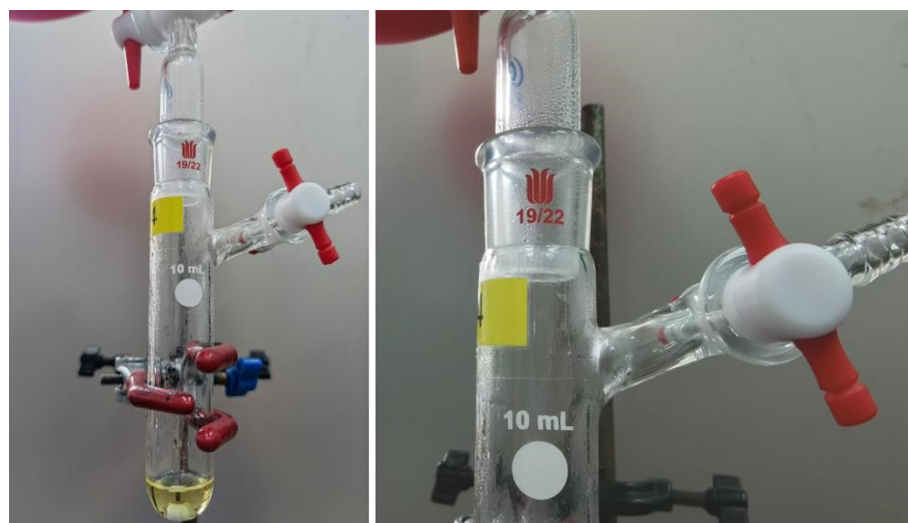


Fig. S14 Condensation phenomenon of styrene oxide in the atmospheric CO₂ cycloaddition reaction.

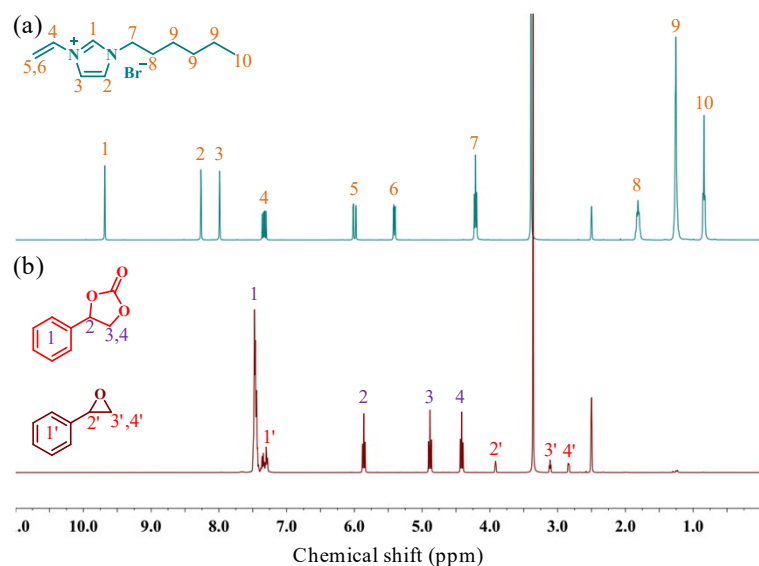


Fig. S15 ¹H NMR spectra (in DMSO-d₆) of (a) [VC6Im]Br and (b) the reaction mixture (Reaction conditions: 12.5 mmol styrene oxide, 1 atm CO₂, 2.5 mol% P-[VC6Im]Br-C8-5%, 80 °C, 36 h.)

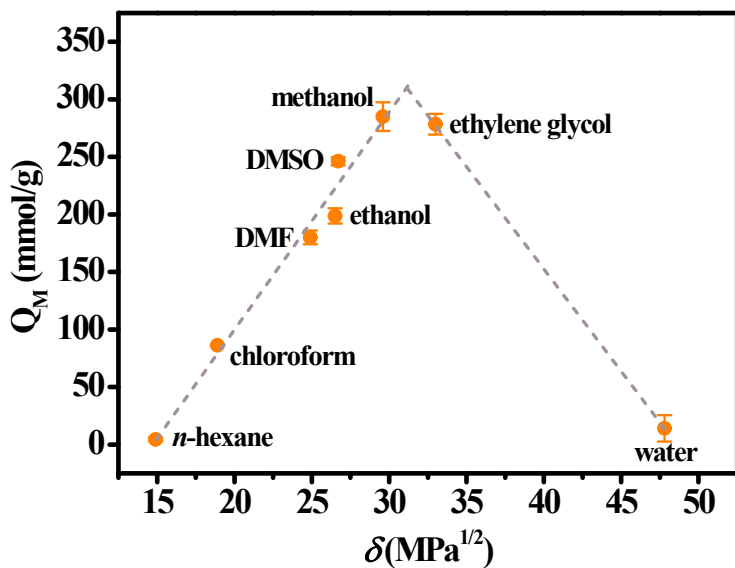


Fig. S16 Relationship between the Q_M value of P-[VC6Im]Br-C8-5% and the solubility parameter (δ) of solvent.

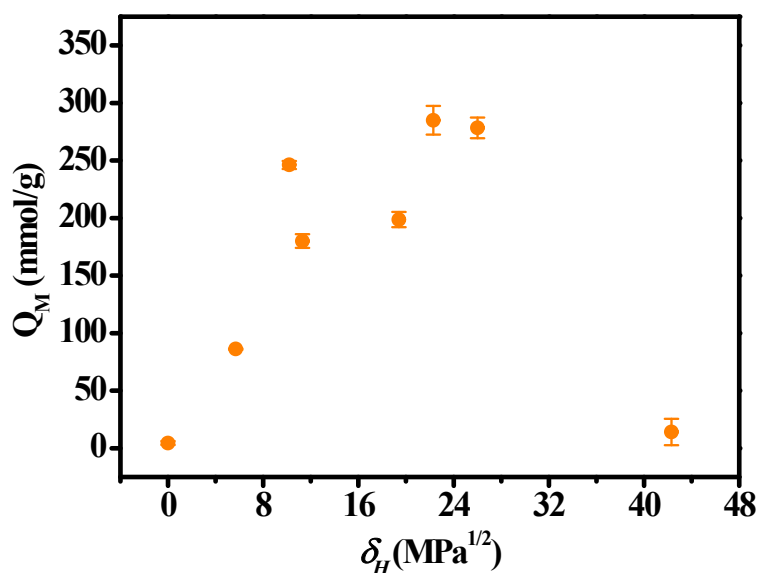


Fig. S17 Relationship between the Q_M value of P-[VC6Im]Br-C8-5% and the Hansen hydrogen-bonding solubility parameter (δ_H) of solvent.

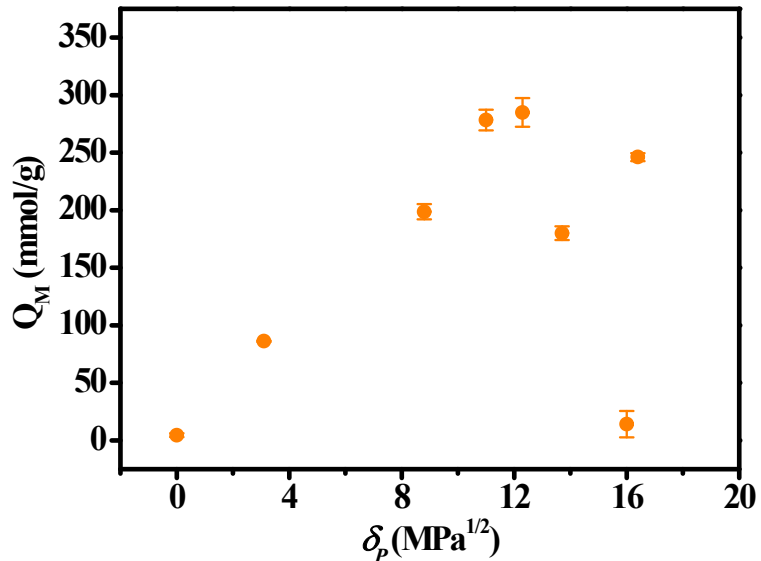


Fig. S18 Relationship between the Q_M value of P-[VC6Im]Br-C8-5% and the Hansen polar solubility parameter (δ_P) of solvent.

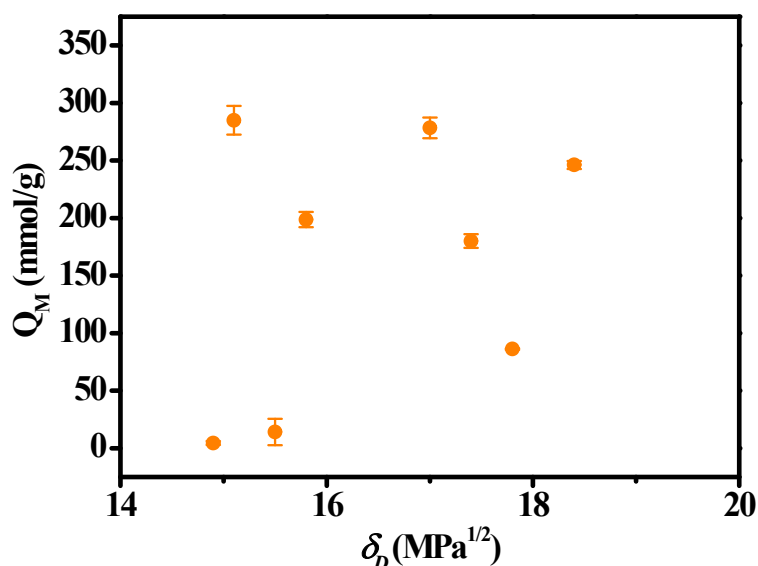


Fig. S19 Relationship between the Q_M value of P-[VC6Im]Br-C8-5% and the Hansen dispersion solubility parameter (δ_D) of solvent.

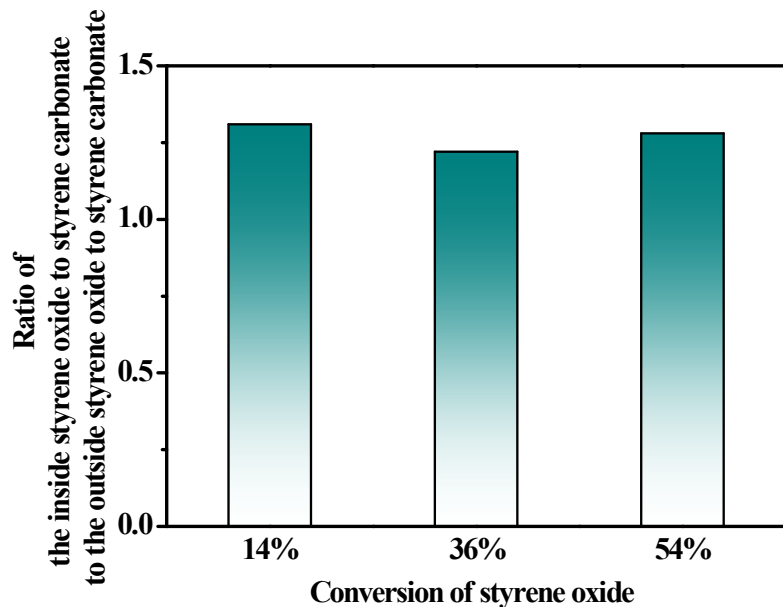
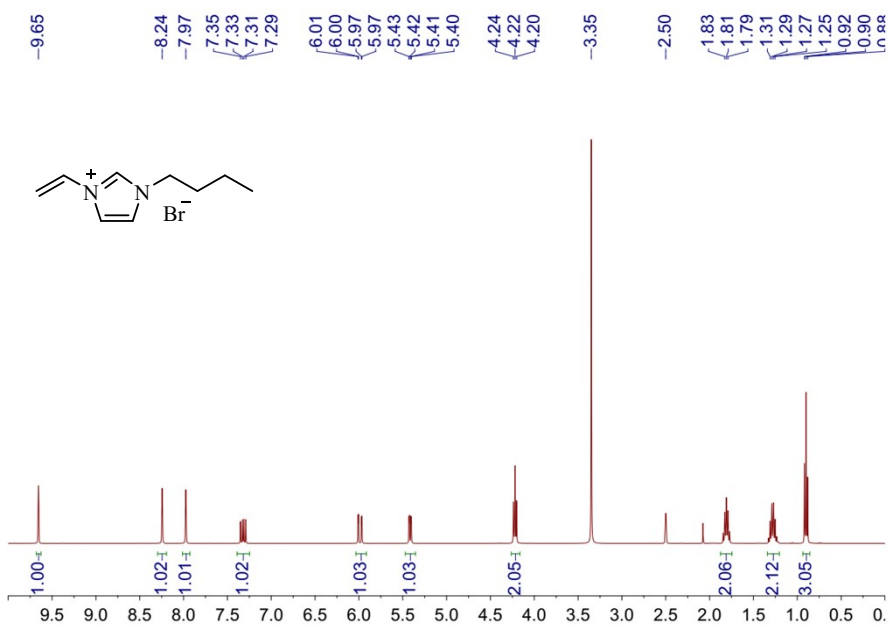


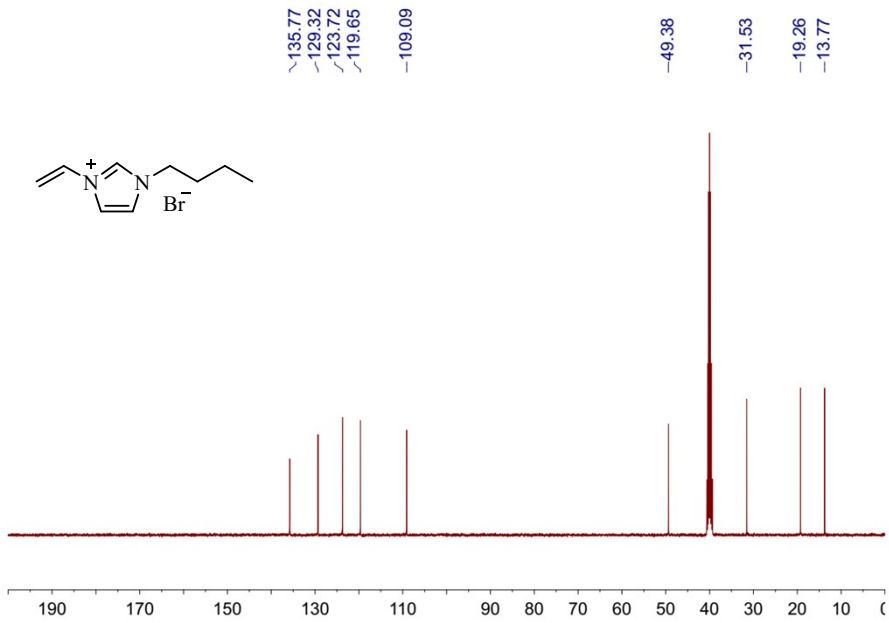
Fig. S20 Ratio of the inside styrene oxide to styrene carbonate to the outside styrene oxide to styrene carbonate in the reaction mixture with different styrene oxide conversion. Reaction conditions: 12.5 mmol styrene oxide, 1 atm (balloon) CO₂, 2.5 mol% P-[VC6Im]Br-C8-5%; 60 °C and 12 h (obtain 14 % conversion), 60 °C and 24 h (obtain 36 % conversion), and 70 °C and 24 h (obtain 54 % conversion).

7. NMR Spectra

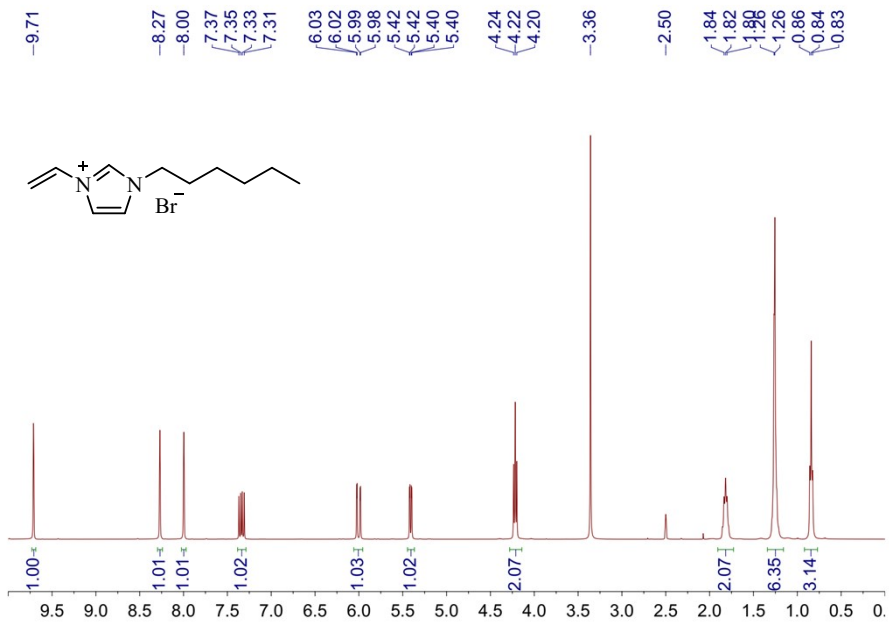
^1H NMR (DMSO-d₆)



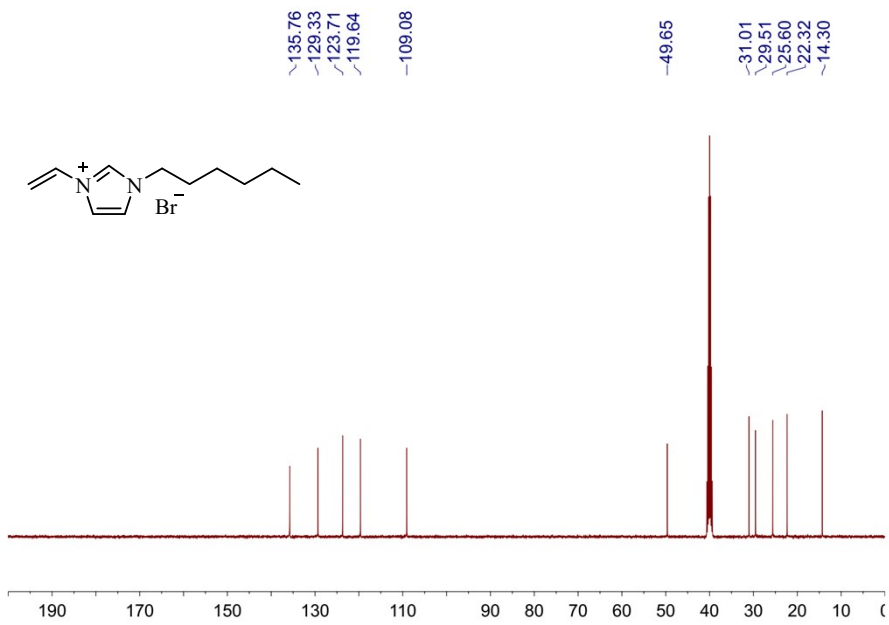
^{13}C NMR (DMSO-d₆)



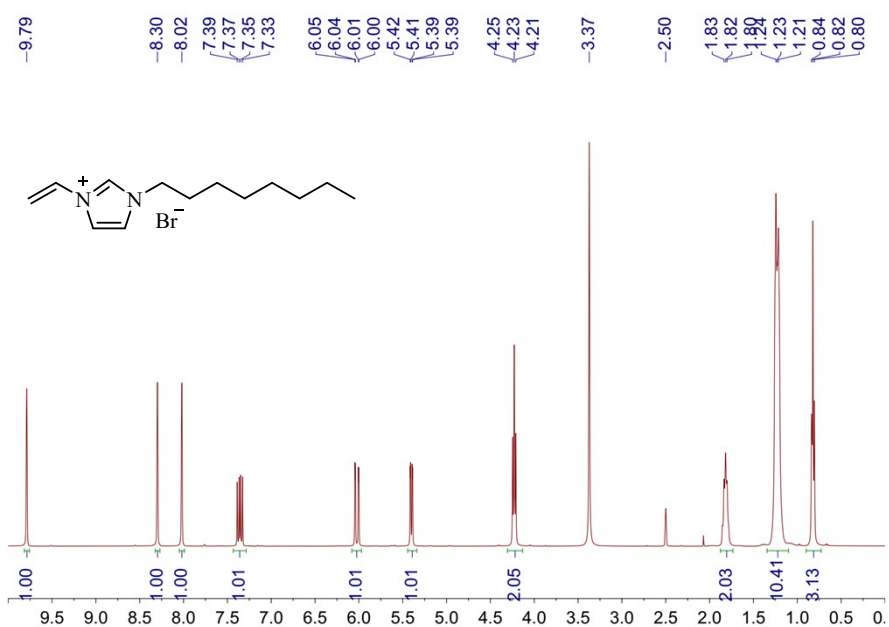
¹H NMR (DMSO-d₆)



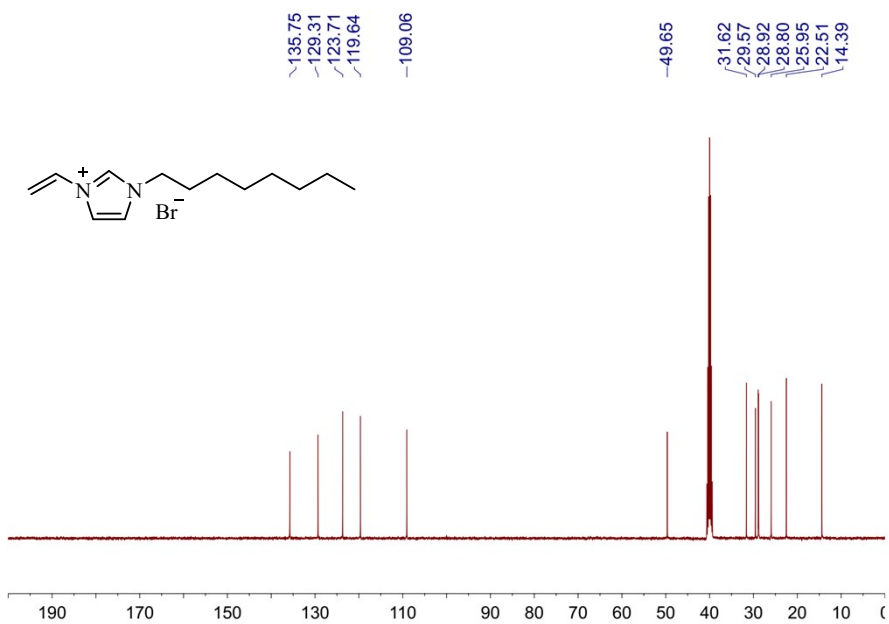
¹³C NMR (DMSO-d₆)



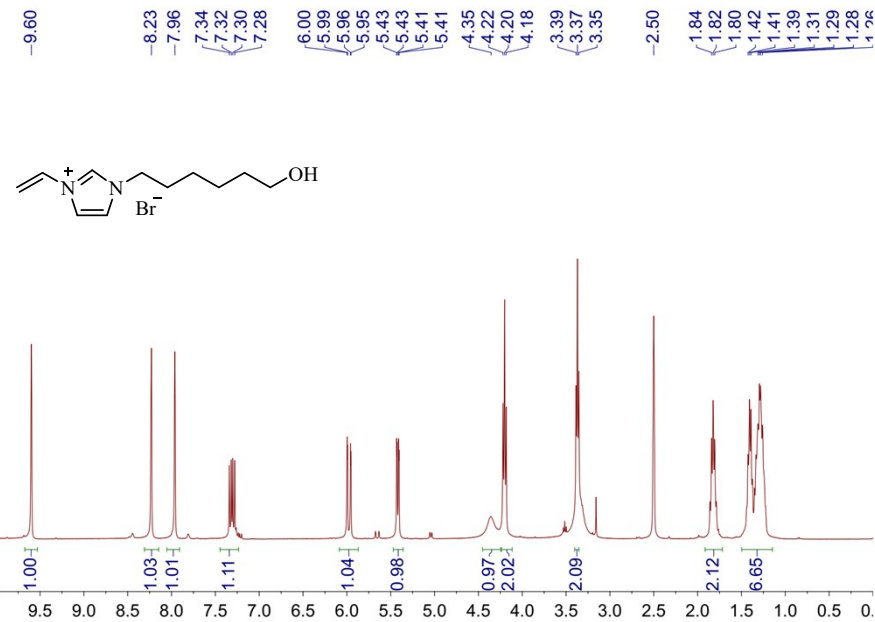
¹H NMR (DMSO-d₆)



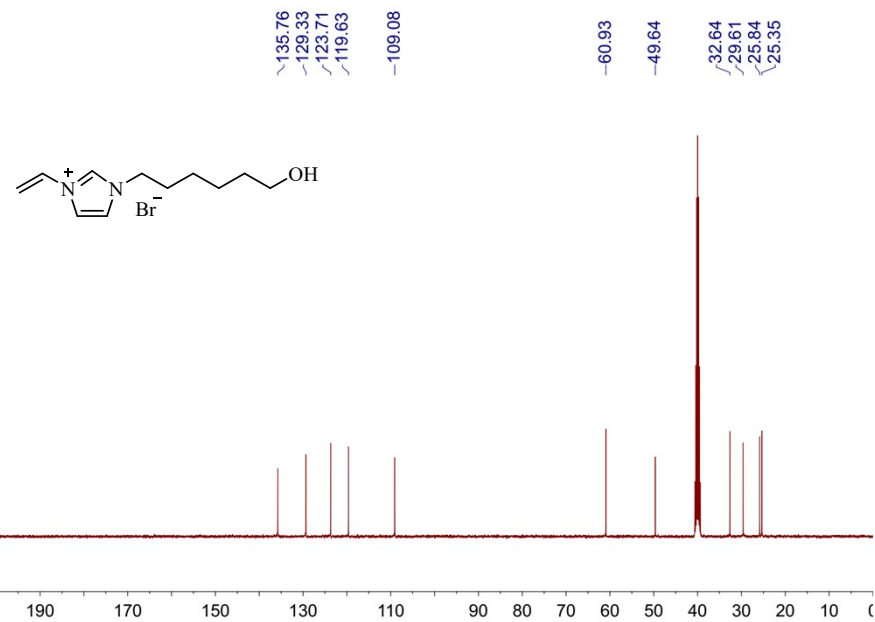
¹³C NMR (DMSO-d₆)



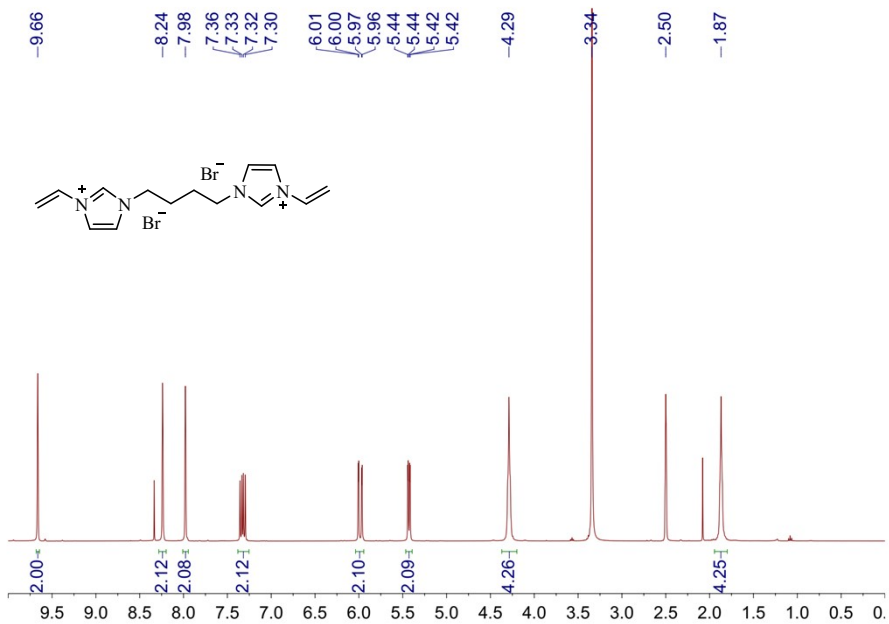
¹H NMR (DMSO-d₆)



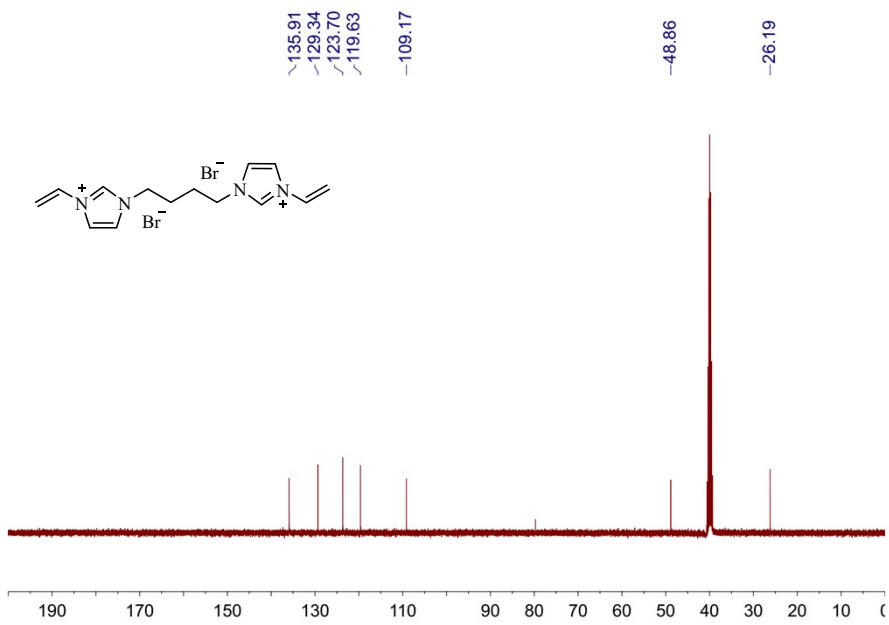
¹³C NMR (DMSO-d₆)



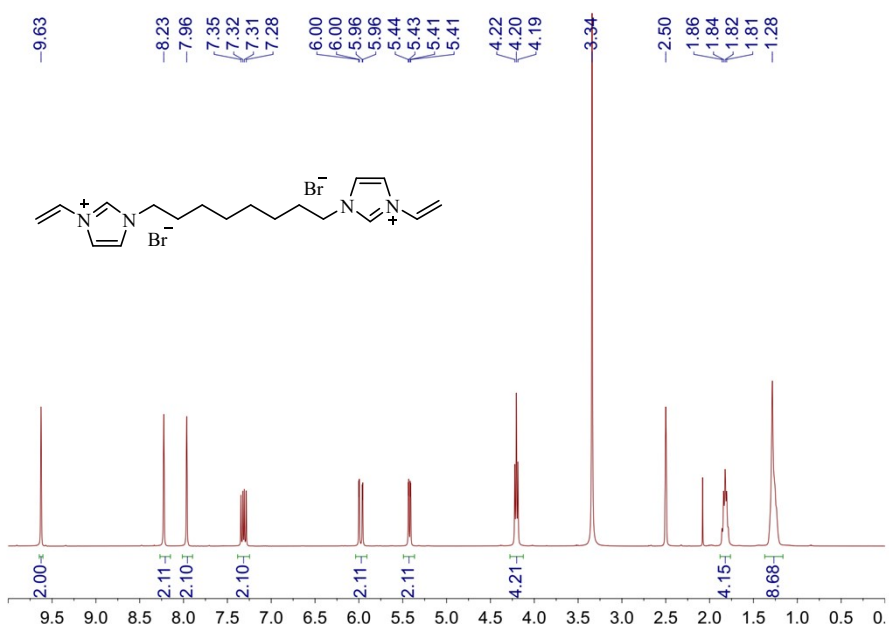
¹H NMR (DMSO-d₆)



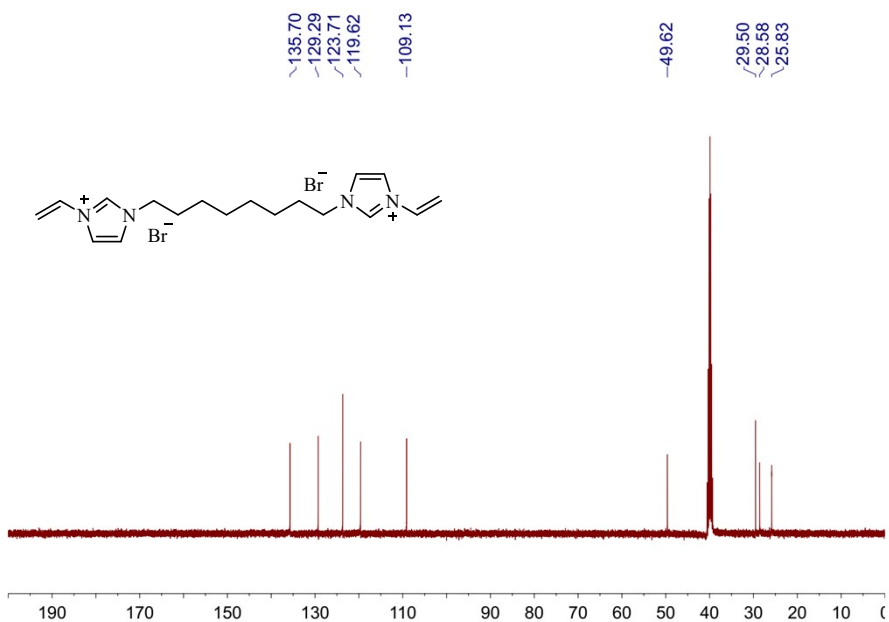
¹³C NMR (DMSO-d₆)



¹H NMR (DMSO-d₆)



¹³C NMR (DMSO-d₆)



8. References

- 1 J. Cui, W. Zhu, N. Gao, J. Li, H. Yang, Y. Jiang, P. Seidel, B. J. Ravoo and G. Li, *Angew. Chem. Int. Ed.*, 2014, **53**, 3844–3848.
- 2 C. M. Hansen, *Hansen Solubility Parameters: A User's Handbook*, 2nd ed., CRC Press, Boca Raton, FL, 2007.